Interpretation of magnetic data using an enhanced local wavenumber (ELW) method

4 authors, including:

Ahmed S. Salem
77 PUBLICATIONS   1,655 CITATIONS

SEE PROFILE

Dhananjay Ravat
University of Kentucky
131 PUBLICATIONS   2,645 CITATIONS

SEE PROFILE

Richard Stuart Smith
Laurentian University
148 PUBLICATIONS   2,220 CITATIONS

SEE PROFILE

Some of the authors of this publication are also working on these related projects:

Project   Masters View project

Project   Reprocessing of Iraq magnetic and gravity data View project

Interpretation of magnetic data using an enhanced local wavenumber (ELW) method

Ahmed Salem[1], Dhananjay Ravat[2], Richard Smith[3], and Keisuke Ushijima[4]

ABSTRACT

This paper presents an enhancement of the local-wavenumber method (named ELW for "enhanced local wavenumber") for interpretation of profile magnetic data. This method uses the traditional and phase-rotated local wavenumbers to produce a linear equation as a function of the model parameters. The equation can be solved to determine the horizontal location and depth of a 2D magnetic body without specifying a priori information about the nature of the sources. Using the obtained source-location parameters, the nature of the source can then be inferred. The method was tested using theoretical simulations with random noise over a dike body. It was able to provide both the location and an index characterizing the nature of the source body. The practical utility of the method is demonstrated using field examples over dikelike bodies from Canada and Egypt.

INTRODUCTION

Developing fully automated techniques for determining generalized source characteristics of magnetic anomalies is a goal of potential-field geophysicists. This has become particularly important recently because large volumes of magnetic data are being collected for environmental and geologic applications. To realize this goal, a variety of semiautomatic methods based on the use of derivatives of the magnetic field have been developed for the determination of magnetic source parameters such as locations of boundaries and depths [e.g., see references in Blakely (1995) and Nabighian and Asten (2002)]. As faster computers and commercial software have become widely available, these techniques are being used more extensively.

One of these techniques is the source parameter imaging (SPI) method (Thurston and Smith, 1997), which requires second-order derivatives of the total field and uses a term known as the local wavenumber to provide a rapid estimate of the depth of buried magnetic bodies. However, the method is model dependent (i.e., it needs information about the nature of the source to estimate the depth). As a result, the accuracy of the depth estimate depends upon how closely the assumed model approximates the real structure. Unfortunately, a priori knowledge of the nature of a source is not usually available.

Recent improvements in the local-wavenumber approach (Smith et al., 1998; Thurston et al., 2002) have made it possible to estimate both the location and nature of the sources. However, the improved methods use third-order derivatives of the field and require data of high quality or careful filtering. Calculation of third-order derivatives from gridded data (Smith et al., 1998) is potentially problematic if data spacing is large in one or more areal dimensions. Salem and Smith (2005) show that normalization of the local wavenumber (by using the value at the anomaly peak) can provide a direct estimation of both the depth and nature of the source. However, their approach requires knowledge of the horizontal position of the source inferred from the peak of the wavenumber profile. Noise can make the selection of this peak location difficult, and inaccuracies in the identified horizontal location will lead to errors in both the estimated depth and information on the nature of the sources.

In this paper, we present an enhancement of the local-wavenumber approach called the enhanced local wavenumber (ELW) method. The ELW method is based on use of the traditional local-wavenumber field and its phase-rotated version, the vertical local-wavenumber field. This combination allows us to calculate the source parameters (for 2D sources)

regardless of their model type. Thus, ELW is a 2D model-independent method and only uses derivatives of the anomalous field up to second order.

ELW METHOD

A local phase is one of three attributes derived from complex analytic signal (Nabighian, 1972) and defined (Thurston and Smith, 1997) as

$$\theta = \tan^{-1}\left(\frac{\partial M/\partial z}{\partial M/\partial x}\right), \tag{1}$$

where $\partial M/\partial x$ and $\partial M/\partial z$ are the derivatives of the magnetic field M in the x and z directions. The rate of change of the local phase θ with respect to the x direction is known as the local wavenumber (Bracewell, 1965) and is expressed (Thurston and Smith, 1997) as

$$k_x = \frac{\partial \theta}{\partial x} = \frac{1}{|A|^2}\left(\frac{\partial^2 M}{\partial x \partial z}\frac{\partial M}{\partial x} - \frac{\partial^2 M}{\partial x^2}\frac{\partial M}{\partial z}\right), \tag{2}$$

where $|A|$ is the amplitude of the analytic signal (Nabighian, 1972) expressed as

$$|A| = \sqrt{\left(\frac{\partial M}{\partial x}\right)^2 + \left(\frac{\partial M}{\partial z}\right)^2}. \tag{3}$$

The local wavenumber k_x over simple bodies (such as contacts, thin dikes, and horizontal cylinders), with horizontal location x_0 and depth z_0, is given (Smith et al., 1998) by

$$k_x = \frac{(\eta + 1)(z_0 - z)}{(x - x_0)^2 + (z - z_0)^2}, \tag{4}$$

where η is a parameter characterizing the source geometry (η is 0 for a contact, 1 for a dike, and 2 for a horizontal cylinder) and is known as the structural index in the Euler method (Thompson, 1982). The classical local-wavenumber approach (the SPI method) is based on equation 4. The depth can only be estimated if the structural index η is known and, as a result, it is a model-dependent method. A simple way to make the method independent in this regard is to find a different local-wavenumber equation that can provide information about either the structural index or the depth. Such an equation can be found by introducing local wavenumbers from higher-order derivatives of the field, similar to Smith et al. (1998) and Thurston et al. (2002). In this study, by incorporating information regarding a phase-rotated version of the local wavenumber, our intent is to provide independent information about the source location as well as the nature of the model without the need for third-order derivatives.

The local phase can be obtained in terms of the structural index by integrating equation 4 with respect to x:

$$\theta = \int_x k_x \partial x = (\eta + 1)\tan^{-1}\left(\frac{x - x_0}{z_0 - z}\right) + C, \tag{5}$$

where C is the constant of integration. Taking the derivative of the local phase θ in the z direction, we obtain the phase-rotated version of the local wavenumber:

$$k_z = \frac{\partial \theta}{\partial z} = \frac{(\eta + 1)(x - x_0)}{(x - x_0)^2 + (z - z_0)^2}. \tag{6}$$

Note that k_x and k_z are a Hilbert transform pair (Bracewell, 1965). The phase-rotated version of the local wavenumber can be calculated from the data in several ways. For example, it can be defined in terms of horizontal and vertical derivatives by taking the derivative of equation 1 in the z direction as

$$k_z = \frac{\partial \theta}{\partial z} = \frac{-1}{|A|^2}\left(\frac{\partial^2 M}{\partial x \partial z}\frac{\partial M}{\partial z} - \frac{\partial^2 M}{\partial z^2}\frac{\partial M}{\partial x}\right). \tag{7}$$

Using the complementary local wavenumbers, k_x and k_z, as above, is what we call here the ELW method. It leads to a solution of the location of the source (x_0 and z_0) simply by dividing equation 4 by equation 6, and then rearranging as

$$k_x x + k_z z = k_x x_0 + k_z z_0. \tag{8}$$

Equation 8 is a simple linear equation; it does not involve η, and can be solved for the source location (x_0, z_0) using conventional methods of matrix inversion. In Appendix A, we describe another way of deriving equation 8 using the Euler method.

SOLUTION STRATEGY

Inversion of equation 8 can be achieved using groups of consecutive observations (windows), and the best solutions can be accepted based on a selection criterion. In this paper, we use only a single window of selected data points close to and centered on the local wavenumber peak k_x location. We suggest a simple strategy to automate the method and reject solutions from false anomalies. In this strategy, the sources are first detected at the locations of the local-wavenumber peaks k_x, using a method of detecting peaks of a field similar to that of Blakely and Simpson (1986). Then the ELW method is applied using a selected number of data points around each peak to estimate the source location parameters (x_0, z_0). The choice of the number of data points to use is a function of the width of the peak, the data quality, and the degree of interference of anomalies from nearby sources. For isolated anomalies, a larger number of data points can be used to overcome the effect of noise. For multiple neighboring sources, a smaller number of data points is appropriate to reduce interference effects. Once the source location (x_0 and z_0) is estimated, a value for the structural index is obtained using equations 4 or 6. The solution is accepted if the estimated index lies close to the range of the 2D magnetic bodies (0–2) (Thompson, 1982; Reid et al., 1990). Noise and errors may shift the indices from the ideal range. Therefore, the acceptance range may be slightly expanded (for example, from −0.2 to 2.2).

THEORETICAL TEST

We demonstrate the feasibility of the present method using synthetic anomaly data of a thin dike model. The dike has a magnetization of 10 A/m produced by an induced field with a declination of 0° and an inclination of 60°. The synthetic anomaly values were calculated on a profile 100-km long at an interval of 1 km. The dike is placed at the center of the profile with its top at a depth of 4 km. Figure 1a shows the calculated total-field anomaly data for the dike model. Figure 1b shows the local-wavenumber fields of the dike model. To ensure the validity of the proposed algorithm, it has been tested using noise-free local-wavenumber fields shown in Figure 1b. In

applying the method, inversion of equation 8 was made using different data points centered above the local-wavenumber peak k_x. For all cases, we found that the method is able to provide the exact values of the horizontal location and depth.

When dealing with real data, noise should be taken into consideration. Noise may lead to errors in the anomaly values that will be mapped into solutions. To test stability of our method in the presence of noise, we contaminated the above total-field anomaly by 1000 different sets of random noise with zero mean and standard deviation of 1 nT. Then, local–wavenumber fields were calculated from the noisy data. Figure 1c shows an example of the local-wavenumber fields after adding the noise. The effect of noise is clearly seen, where both the local-wavenumber anomalies (k_x and k_z) of the dike are destroyed and several false anomalies are created. This is not surprising, as the local-wavenumber anomalies require calculation of the second-order derivatives of the field, which enhance the noise. The method was applied to the noisy local-wavenumber data using the above strategy. We used a single window of 21 data points to estimate the source location from equation 8. Then, for each source location solution, a value of the structural index was obtained using equation 6. We examined structural indices from both equations 4 and 6, and found that the latter one gives slightly better results. Solutions were rejected if their estimated indices were outside the acceptance range (-0.2 to 2.2). This strategy robustly yielded solutions only for the true k_x peak of the dike model. Figure 1d shows the estimated source parameters from the noisy local-wavenumber data for the used model; the statistics of the results are listed in Table 1. The maximum depth error is less than 0.6 km. As it can be seen, without applying any enhancement or smoothing techniques, the results are all close to the actual model parameters and indicate the robustness of the present method. Fortunately, the noise level of modern aeromagnetic surveys has become very low and, thus, the method should provide good results from field data of reasonable resolution.

APPLICATION TO FIELD DATA

Example from Canada

Figure 2a shows part of an aeromagnetic flight line over a magnetic body in the Matheson area of northern Ontario, Canada. The magnetic sensor was located in a bird about 70 m above the ground, and the station spacing was approximately 12 m (Ontario Geological Survey, 2000). The survey was flown N30°W, which is perpendicular to the geologic strike. The magnetic anomaly seen near 700 m in Figure 2a has been drilled, and the depth to the top of the

magnetic body is 41 m below surface. The local-wavenumber fields (Figure 2b) display several false anomaly peaks caused by high-frequency noise. The local-wavenumber peaks were detected, and the ELW method was applied to estimate the source parameters using the strategy of rejecting false peaks as in the synthetic-noise test example and using a single window of 21 data points. Results of the ELW method indicate that a source at a horizontal location of 725.2 ±1.1 m, a depth of 139.6 ±2.6 m, and a structural index of 1.13 ±0.04 explains the observed data. The error bars on the estimated parameters in this and later examples are from associated standard deviations that were obtained from the covariance matrix of the estimated parameters (Meju, 1994). The estimated structural index is close to 1 and indicates that the source is a dikelike body. The estimated depth is slightly deeper than the actual source-to-observation distance (111 m). Vallee et al. (2004) showed that theoretical data from a dike source located at a
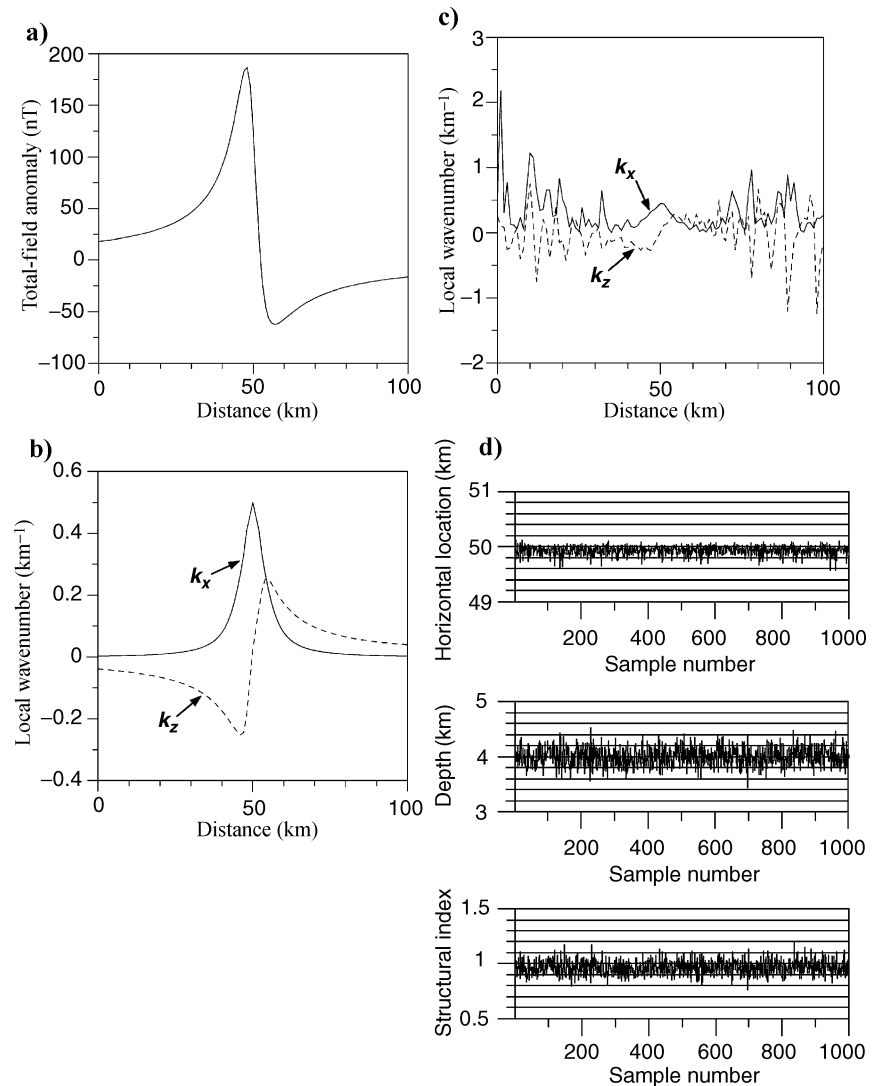

Figure 1. (a) Total-field anomaly for a dike model at a horizontal location of 50 km and a depth of 4 km. (b) Local-wavenumber fields of the data of (a). (c) An example of local-wavenumber fields after adding random noise with zero mean and a standard deviation of 1 nT to the data of (a). (d) Estimate of the horizontal location, depth, and structural index from a set of 1000 different noisy local-wavenumber fields of the data of (a).

depth of 143 m match the observed magnetic anomaly. Thus, it seems that the errors in the derived source parameters are likely to be caused by small deviations of the source from an assumed idealized geometry and possibly also caused by noise.

Table 1. Results of testing the ELW method with anomaly data of Figure 1a after adding 1000 different sets of random noise with zero mean and standard deviation of 1 nT.

	Minimum	Maximum	Average	Standard deviation
Horizontal location (km)	49.57	50.11	49.93	0.07
Depth (km)	3.44	4.52	4.00	0.16
Structural index	0.76	1.20	0.97	0.06

EXAMPLE FROM EGYPT

Figure 3a shows a section from high-resolution airborne magnetic data over Hamrawien area, western margin of the Red Sea, Egypt. The airborne survey was conducted along a set of parallel lines directed N60°E. A cesium magnetometer with a sensitivity of 0.001 nT was used (Salem et al., 1999). The section was flown at an average terrain clearance of 150 m with a sampling interval of approximately 10 m. The area largely covers metavolcanic and sedimentary rocks. Generally, the magnetic field over the sedimentary and metavolcanic rocks in this area takes the form of low-amplitude, long-wavelength variations on which a number of high-amplitude, short-wavelength anomalies are superimposed. Two of these high-amplitude anomalies are clearly seen in the observed data (Figure 3a). Figure 3b shows the calculated local-wavenumber fields of the observed magnetic data. Unlike the total-field data, the local-wavenumber data display several peaks.
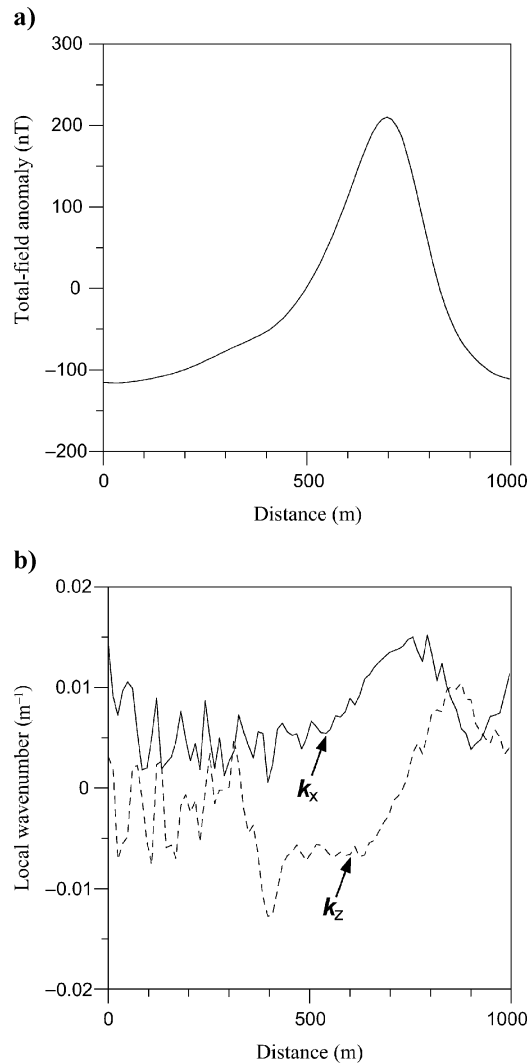

Figure 2. (a) A section of airborne magnetic anomaly over a dike body in the Matheson area, Canada. (b) Local-wavenumber fields of the data of (a).
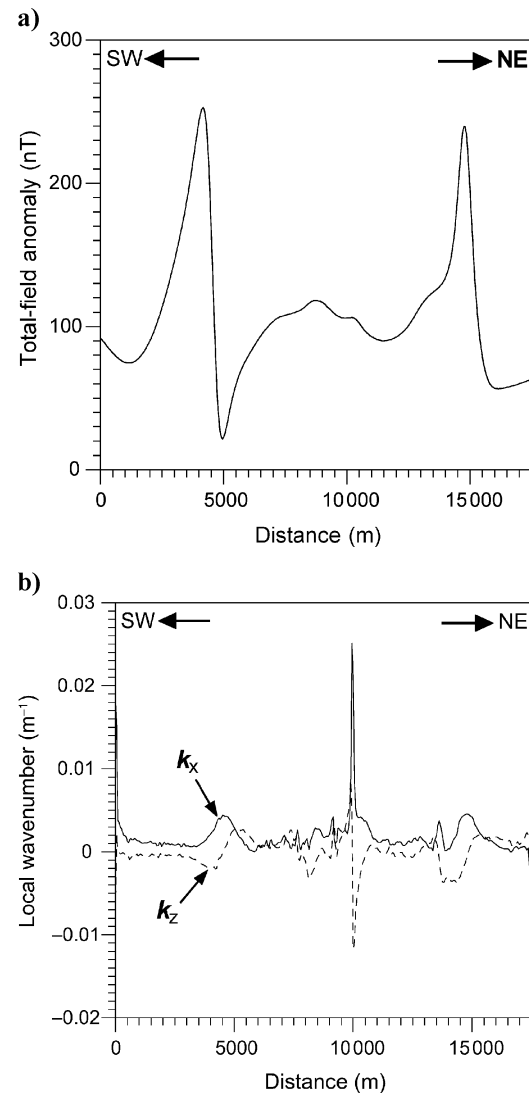

Figure 3. (a) A section of airborne magnetic anomaly data over unknown sources in Hamrawien area, western margin of the Red Sea, Egypt. (b) Local-wavenumber fields of the data of (a).

In applying the method, the local wavenumber peaks of k_x were first detected and inversion was employed using a single window of 21 data points centered over each detected peak. Using our strategy, only two solutions were acceptable, and they are associated with the southwestern and northeastern anomalies shown in Figure 3a. Solutions for the peaks near the central part of the section were rejected because their estimated indices were outside the acceptance range (-0.2 to 2.2). These peaks are most probably caused by noise or very deep sources for which 2D assumption would not be valid. The accepted solutions indicate that the southwestern anomaly can be explained by a source located at a horizontal distance of 4526.3 ± 7 m, a depth of 555.7 ± 10 m, and a structural index of 1.44. On the other hand, the northeastern anomaly can be produced by a source located at a horizontal distance of $14\,858.4 \pm 17$ m, a depth of 441.2 ± 13 m, and a structural index of 1.20. The estimated structural-index values indicate that the sources are most probably dikes. The high amplitude of their magnetic anomalies suggests that these dikes were formed by diabasic materials associated with the Red Sea rifting (Salem et al., 2000). There is no drilling information to verify the results of this example. However, we cor-roborate the results with the results of the AN-EUL method (Salem and Ravat, 2003). AN-EUL combines the analytic signal and Euler method, and provides depth and a structural index at the location of the analytic-signal maxima. Following Salem and Ravat (2003), we applied the AN-EUL method after upward continuing the data starting with different heights (ranging from 50 to 300 m) and using an interval of 50 m. For all levels, maxima of the analytic signal were found at horizontal distances of 4500 m for the southwestern anomaly and 14 850 m for the northeastern anomaly. Figures 4a and 4b show the estimate of the depth and structural index for the southwestern anomaly and the northeastern anomaly, respectively. Generally, starting from the upward-continuation distance of 100 m, results of AN-EUL method become stable and are close to the results of the ELW method. However, because the ELW method requires only second-order derivatives of the field and is employed in the least-square sense, we think that good results can be obtained from routine field data of reasonable quality without applying any enhancement or smoothing techniques.

CONCLUSION

In this paper, we present a new technique, the enhanced local-wavenumber (ELW) method, for the interpretation of magnetic data across 2D sources that uses simultaneously two complementary first-order local wavenumbers. The ELW method yields a linear equation to estimate the horizontal location and depth of 2D magnetic sources without a priori information about the nature of the sources. Information about the nature of the sources is subsequently obtained by finding structural indices using the estimated source location parameters. The ELW method was tested using synthetic anomaly data with and without random noise. The method was also tested using field magnetic anomaly data over a magnetic body of known source parameters from drilling. In synthetic cases, the method estimated the source parameters with adequate precision. For the field example, the results agree with the drilling results. The utility of the method is also demonstrated using high-resolution magnetic data over unknown magnetic sources in Hamrawien area, western margin of the Red Sea, Egypt. The results of the ELW method were found to be in agreement with the results of the AN-EUL method.

APPENDIX A

RELATION BETWEEN THE ELW AND THE EULER METHODS

The 2D form of Euler's equation can be defined (Thompson, 1982) (with the same notation as in the main text) as

$$(x - x_o)\frac{\partial M}{\partial x} + (z - z_o)\frac{\partial M}{\partial z} = -\eta M. \qquad \text{(A-1)}$$
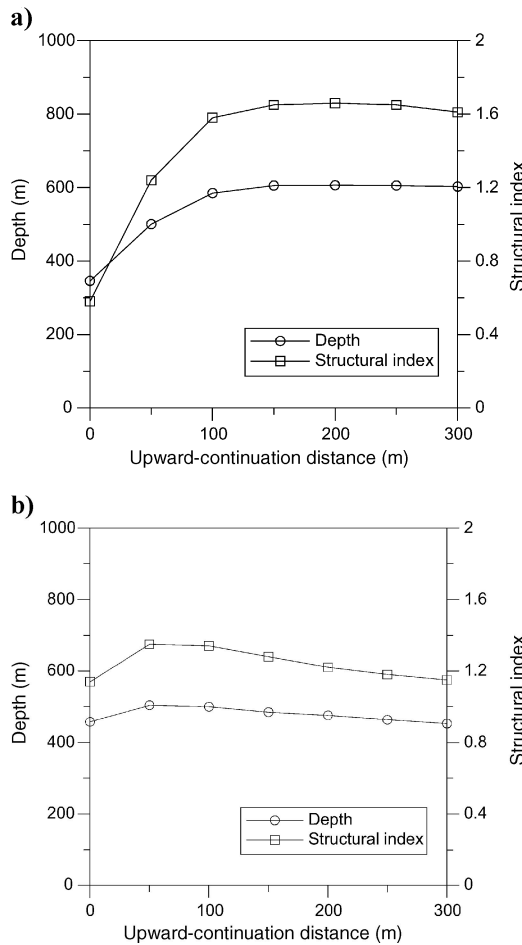

Figure 4. (a) Results of the AN-EUL method for the southwestern anomaly of Figure 3a with different upward-continuation distances. (b) Results of AN-EUL method for the northeastern anomaly of Figure 3a with different upward-continuation distances.

Taking the derivatives of the Euler equation A-1 in the x and z directions, we obtain

$$(x - x_o)\frac{\partial^2 M}{\partial x^2} + (z - z_o)\frac{\partial^2 M}{\partial z \partial x} = -(\eta + 1)\frac{\partial M}{\partial x} \quad \text{(A-2)}$$

and

$$(x - x_o)\frac{\partial^2 M}{\partial x \partial z} + (z - z_o)\frac{\partial^2 M}{\partial z^2} = -(\eta + 1)\frac{\partial M}{\partial z}. \quad \text{(A-3)}$$

Multiplying equations A-2 and A-3 by $[(1/|A|^2)(\partial M/\partial z)]$ and $[(1/|A|^2)(\partial M/\partial x)]$, respectively, followed by subtraction, we obtain

$$\frac{(x - x_0)}{|A|^2}\left(\frac{\partial^2 M}{\partial x \partial z}\frac{\partial M}{\partial x} - \frac{\partial^2 M}{\partial x^2}\frac{\partial M}{\partial z}\right)$$
$$= \frac{(z - z_0)}{|A|^2}\left(\frac{\partial^2 M}{\partial x \partial z}\frac{\partial M}{\partial z} - \frac{\partial^2 M}{\partial z^2}\frac{\partial M}{\partial x}\right). \quad \text{(A-4)}$$

Rearrangement of equation A-4 in terms of k_x and k_z yields

$$k_x x + k_z z = k_x x_0 + k_z z_0, \quad \text{(A-5)}$$

where

$$k_x = \frac{1}{|A|^2}\left(\frac{\partial^2 M}{\partial x \partial z}\frac{\partial M}{\partial x} - \frac{\partial^2 M}{\partial x^2}\frac{\partial M}{\partial z}\right) \quad \text{(A-6)}$$

and

$$k_z = \frac{-1}{|A|^2}\left(\frac{\partial^2 M}{\partial x \partial z}\frac{\partial M}{\partial z} - \frac{\partial^2 M}{\partial z^2}\frac{\partial M}{\partial x}\right) \quad \text{(A-7)}$$

are the two perpendicular local wavenumbers.

REFERENCES

Blakely, R. J., 1995, Potential theory in gravity and magnetic applications: Cambridge University Press.

Blakely, R. J., and R. W. Simpson, 1986, Approximating edges of source bodies from magnetic or gravity anomalies: Geophysics, **51**, 1494–1498.

Bracewell, R., 1965, The Fourier transform and its applications: McGraw-Hill Book Co.

Meju, M. A., 1994, A general program for linear parameter estimation and uncertainty analysis: Computers & Geosciences, **20**, 197–220.

Nabighian, M. N., 1972, The analytic signal of two-dimensional magnetic bodies with polygonal cross-section: Its properties and use for automated anomaly interpretation: Geophysics, **37**, 507–517.

Nabighian, M. N., and M. Asten, 2002, Metalliferous mining geophysics: State of the art in the last decade of the 20th century and the beginning of the new millennium: Geophysics, **67**, 964–978.

Ontario Geological Survey, 2000, Ontario airborne geophysical surveys, magnetic and electromagnetic data, Matheson area: Geophysical Data Set 1101.

Reid, A. B., J. M. Allsop, H. Granser, A. J. Millet, and I. W. Somerton, 1990, Magnetic interpretation in three dimensions using Euler deconvolution: Geophysics, **55**, 80–91.

Salem, A., and D. Ravat, 2003, A combined analytic signal and Euler method (AN-EUL) for automatic interpretation of magnetic data: Geophysics, **68**, 1952–1961.

Salem, A., and R. S. Smith, 2005, Depth and structural index from the normalized local wavenumber of 2D magnetic anomalies: Geophysical Prospecting, **51**, 83–89.

Salem, A., A. Elsirafi, and K. Ushijima, 1999, Design and application of high-resolution aeromagnetic survey over Gebel Duwi area and its offshore extension, Egypt: Memoirs of the Faculty of Engineering, Kyushu University, **59**, no. 3, 201–213.

Salem, A., K. Ushijima, A. Elsirafi, and H. Mizunaga, 2000, Spectral analysis of aeromagnetic data for geothermal reconnaissance of Quseir area, northern Red Sea, Egypt: Proceedings of World Geothermal Congress 2000, 1669–1673.

Smith, R. S., J. B. Thurston, T. Dai, and I. N. MacLeod, 1998, iSPI—The improved source parameter imaging method: Geophysical Prospecting, **46**, 141–151.

Thompson, D. T., 1982, EULDPH, A new technique for making computer-assisted depth estimates from magnetic data: Geophysics, **47**, 31–37.

Thurston, J. B., and R. S. Smith, 1997, Automatic conversion of magnetic data to depth, dip, and susceptibility contrast using the SPI method: Geophysics, **62**, 807–813.

Thurston, J. B., R. S. Smith, and J. Guillon, 2002, A multimodel method for depth estimation from magnetic data: Geophysics, **67**, 555–561.

Vallee, M. A., P. Keating, R. S. Smith, and C. St.-Hilaire, 2004, Estimating depth and model type using the continuous wavelet transform of magnetic data: Geophysics, **69**, 191–199.